Pergamon

Solar Energy, Vol. 52, No. 3, pp. 289–300, 1994

0038-092X/94 $6.00 + .00

FLOW DISTRIBUTION IN MANIFOLDED SOLAR COLLECTORS WITH NEGLIGIBLE BUOYANCY EFFECTS

G. F. JONES** and NOAM LIOR*‡
** Department of Mechanical Engineering, Villanova University, Villanova, PA 19085, U.S.A.
‡ Department of Mechanical Engineering and Applied Mechanics, University of Pennsylvania, Philadelphia, PA 19104-6315, U.S.A.

Abstract—To understand the influence of collector design parameters on the flow distribution among the solar collector absorber tubes, and as a first step to any detailed analysis of the influence of flow on heat transfer in the collector and on its consequent thermal performance, this study investigates the distribution of flow through a typical system consisting of two manifolds connected by a number of parallel riser tubes. No thermal effects, such as buoyancy, are taken into account. A discrete hydrodynamic model was developed for this system, and the resulting set of simultaneous nonlinear algebraic equations was solved numerically for 54 different combinations of the major independent variables. Quantitative flow distribution results are presented. In the investigated range, it was determined that the three parameters which have the major influence on flow distribution are, in the order of significance, the ratio of riser diameter to manifold diameter, the number of risers, and the length of the risers, with maldistribution increasing with the increase of the first two and with the decrease of the third one. To demonstrate the most dramatic influence, changing the value of d_r/d_i from 0.25 to 0.75 causes the peak riser flow excess above the average flow to increase 100-fold: from 5% for the first diameter ratio, to 500% for the second. Consistent with his finding, pressure changes in the system arising from inertia in the manifolds become larger than the frictional pressure changes in the risers when the riser tube length-to-diameter is decreased below about 75, causing large flow maldistribution. Predictions from the model are successfully compared with limited experimental data and with the closed-form solutions of two existing models.

1. INTRODUCTION

The thermal performance of flat plate solar collectors depends on the local internal flow rates of the heated fluid distributed through the tubes attached to (or integrated within) the absorber plate, as well as through the individual collectors in a collector bank piped in parallel by common manifolds. The few studies performed on this subject so far have conclusively shown, by comparison with experiments, field data, and the predictions of the Hottel–Whillier model (which assumes uniform absorber temperature), that collector or collector-array efficiency decrease as the uniformity of flow distribution diminishes[4,8,10,12,16,18,22].

Very little, basically contained in the articles by Dunkle and Davey[10], Jones and Lior[13,14], Menuchin *et al.*[18], Wang and Yu[21], and Wang and Wu[22], has been published on the prediction of flow distribution in solar collectors and on the sensitivity of the flow distribution to the collector design parameters. The flow distribution in solar collectors is somewhat affected by the thermal conditions, through the advent of buoyancy-driven flows and through temperature dependence of the thermophysical properties. As addressed by our past work[13], these effects complicate the analysis significantly, but have negligible influence on collector efficiency when the heat transfer coefficients and Peclet numbers in the risers are large, as they usually are in solar collectors (cf. Jones[14]). The objective of this study is to present, as a first step, an appropriate, experimentally validated isothermal model and to provide a sensitivity analysis and design recommendations for conditions typical of solar collectors in the which the fluid is distributed through a manifold system. If the temperature rise in the collector is relatively small, as it often is in practice, an isothermal analysis may be of sufficient accuracy even without correction for thermal effects.

Past flow distribution work has focused on single manifolds in combining or dividing flow and on connected combining and dividing manifolds (hereafter an assembly of parallel risers connected by outlet and inlet manifolds would be referred to as a "dual-manifold system"). The results of the analysis for the latter geometry can be applied directly to solar collector work.

The fluid mechanics of flow branching are well understood in principle (cf. McNown[17], Acrivos *et al.*[1], Dunkle and Davey[10], Bajura[2], Bajura and Jones[3], Datta and Majumdar[9], Pigford *et al.*[19], Bassiouny and Martin[5,6], Hager[11], Shen[20]). The dual-manifold system geometry considered here is shown in Fig. 1. Briefly, as the fluid passes through a branch region in the inlet manifold, mass and momentum conservation require that the downstream velocity decreases and pressure increases. The increase in pressure is then offset to some extent by frictional

* ISES member.

effects which occur in the length of manifold that connects two adjacent branch regions. In the outlet manifold both the combining flow from the risers and the frictional losses in nonbranch regions cause a decrease in pressure in the direction of flow. Finally, an energy balance on each riser tube requires that the flow rate be related to the difference in pressure between the inlet and outlet manifolds at the location where the riser is connected to them.

In the past, two analytical approaches have been taken to describe the flow distribution process at a branch region:

1. *Differential*—where the simplifying assumption of continuous removal (or addition) of flow from (or to) the manifolds through a porous strip or slot running along the entire inlet and outlet manifolds is made (cf. Bajura[2], Bajura and Jones[3], Datta and Majumdar[9], Bassiouny and Martin[5,6], Hager[11], Shen[20]).
2. *Discrete*—where flow is assumed to be removed (or added) at specific locations (at which the risers are connected) along both manifolds, as it occurs in reality (cf. Jones and Lior[12], Acrivos *et al.*[1], Pigford *et al.*[19]).

The advantage of the continuous over the discrete formulation is the possibility of getting analytical solutions, and specifically the ease by which bounding solutions to limiting cases can be found in terms of elementary functions. In addition, the problem of determining accurate pressure regain coefficients, which are required for the discrete formulation, can possibly be eliminated. Although this type of formulation is usually adequate to indicate general trends in many types of practical collector designs, the results may not be quantitatively valid since usually the number of risers is relatively small. In the work by Acrivos *et al.*[1]the problem was approached with a discrete model applicable only to single combining or dividing manifolds.

Specifically related to flow distribution in solar collectors, Dunkle and Davey[10]have analyzed it using the continuous formulation. They found experimentally that peak collector fluid temperatures 50% greater than outlet temperatures can be realized in collector banks due to unequal cooling caused by nonuniform flow distribution, with a subsequent anticipated reduction in collector thermal efficiency. Discrete formulations of the problem are only those by the authors and later by Wang and coworkers: Jones and Lior[12]developed and analyzed the results of a discrete model for isothermal flow in solar collector dual manifolds, which is the basis for this article; using the model of Jones and Lior, Wang and Yu[21]have successfully compared the predictions of the model to experimental observations of pressure distributions reported 14 years earlier by others. They have also used the model to conduct an analysis of the sensitivity of maldistribution to the major geometric and flow parameters of the system, and to the pressure-regain and energy-loss coefficients. Most of their results are in agreement with those of the previously published literature, with the exception of a puzzling experimental result showing that the pressure difference across most of the risers is zero, indicating no flow in these risers. No description is given of the experimental technique used, and an instrumentation/measurement error is likely when measuring the very small pressure differences along the manifolds.

Also based on the Jones and Lior[12]model for flow distribution in a single collector, Menuchin *et*

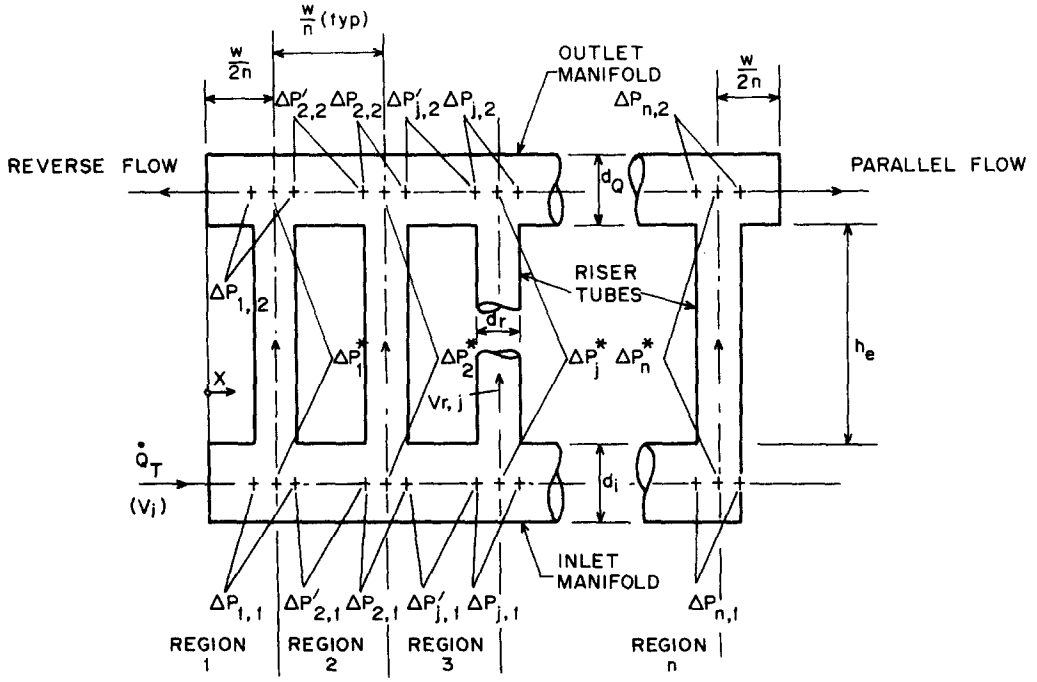

Fig. 1. Schematic for the dual-manifold system hydrodynamic model.

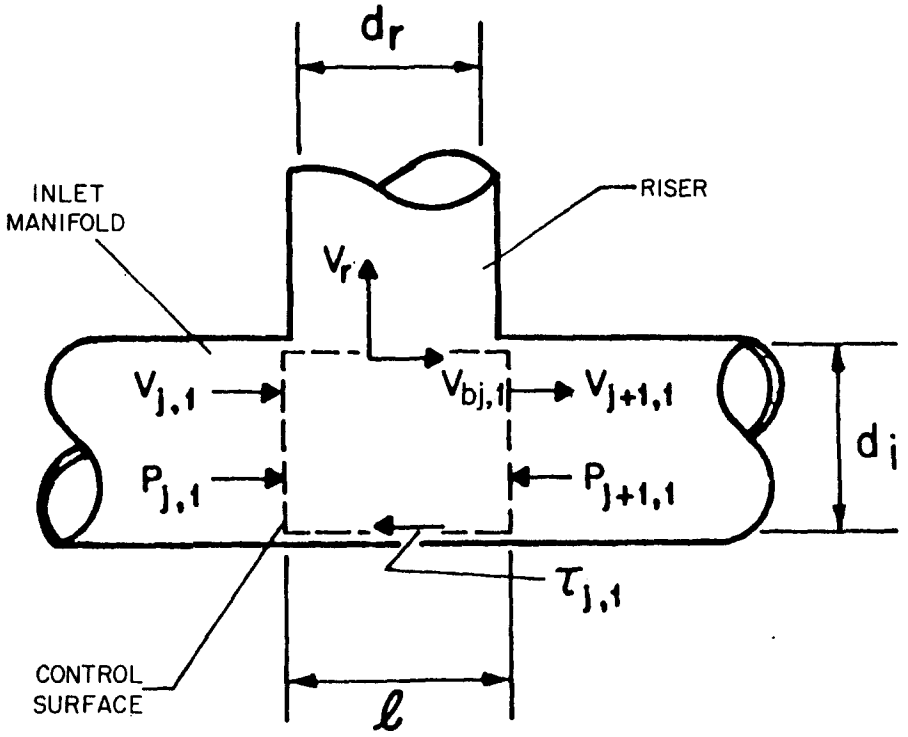

Fig. 2. Momentum balance in single branch of inlet manifold.

al.[18]computed the effects of flow distribution and of other parameters on parallel- and series-piped solar collector arrays. More recently, Wang and Wu[22] developed a simplified and less general thermal performance model for parallel-piped solar collectors having common manifolds (this is one of the ways to parallel-pipe an array) and at least partially verified it by experiments using 16 collectors each having 10 risers. They found strong maldistribution in this array, with almost all of the flow passing just through the first and last collector when a parallel-flow configuration ("Z"-array) was used, and almost all of the flow passing through the first collector when a reverse-flow configuration ("C"-, or "U"-array, the parallel-flow configuration is sometimes referred to as "reverse return," and the reverse configuration as "direct return.") was used. As mentioned above, this flow maldistribution and the effect of heat transfer to the manifolds were found by them to cause an efficiency drop of about 40% when compared to the predictions of the Hottel–Whillier model. Clearly, such high maldistribution is undesirable, and indeed most array designers know better than to pipe the collectors in the way done in these experiments. Remarkably, their experiments have shown that the pressure in the outlet manifold was higher than that in the inlet manifold in all but the two end collectors in the Z configuration, and in all but the first collector in the U configuration, a phenomenon which the authors speculatively attributed to natural convection effects. This observation is highly unlikely in our opinion, and probably is due to systematic instrumentation or measurement error.

It is clear that a more definitive and accurate study and modeling of flow distribution in typical solar collectors, to determine which of the collector design variables influence flow distribution and at the same time to specify values for those variables which ensure minimal flow maldistribution, is necessary. This study addresses these objectives.

2. THE HYDRODYNAMIC MODEL

Consider the case of one-dimensional, incompressible, isothermal forced flow of a fluid passing through a branch region as shown in Fig. 2 for a dividing branch of the manifold depicted in Fig. 1. The configuration and notations for a combining branch are analogous. Since, as described above, detailed models of general manifold flow distribution are available in the literature, only a brief description of the model presented in this article is given below.

The first two modeling assumptions stated above are admissible for low speed liquid flow within straight and relatively small-diameter flow passages. The third assumption permits the effect of density and transport property variations caused by temperature gradients within the fluid to be ignored. Usually the most serious errors that this assumption generates is that it ignores the effect of buoyancy on the flow distribution, which may become important in solar collectors that are not horizontal in a gravity field and are operated with small fluid flow rates. In such cases this assumption generates solutions which predict the highest maldistribution because the flow-starved risers will, in general, become

warmer than the others, giving rise to onset of natural convection inside the tubes, which would then tend to diminish the flow maldistribution to some extent. The solution of the nonisothermal problem with buoyancy effects is significantly more complex and is beyond the scope of this study; a specific solution presenting some limiting cases was developed by the authors (Jones and Lior[13]).

Referring to the symbols in Fig. 2 and adding the assumption that the diameters of the inlet and outlet manifolds are the same ($d_o = d_i$) and that $\ell = d_r$, the momentum equation for a branch control volume is written as

$$\frac{\Delta P_{j,1}}{\rho} = V_{j+1,1}^2 - V_{j,1}^2 + V_{bj,1}V_{r,j}\left(\frac{d_r}{d_i}\right)^2 + \alpha_{j,1}(V_{j,1}^2 + 2V_{j,1}V_{j+1,1} + V_{j+1,1}^2), \quad (1a)$$

where the third term on the right accounts for the loss of momentum in the manifold from the flow branching to the riser. The last term on the right accounts for friction in the branch assuming that the characteristic velocity is the mean of the branch upstream and downstream values. The surface area of the branch is taken as the surface area of the manifold less that due to the connection with the riser. In eqn (1a), all velocities are assumed to be cross-sectionally uniform. Any deviations from this last assumption will be accounted for in the empirical pressure regain coefficients discussed below.

In dimensionless form, the momentum and mass conservation equations are written for each branch control volume, as

$$\Delta\hat{P}_{j,1} = (1 + \alpha_{j,1})\hat{V}_{j+1,1}^2 - (1 - \alpha_{j,1} - \gamma_i) \times \hat{V}_{j,1}^2 - (\gamma_i - 2\alpha_{j,1})\hat{V}_{j,1}\hat{V}_{j+1,1}, \quad (1b)$$

$$\hat{V}_{j+1,1} = \hat{V}_{j,1} - \left(\frac{d_r}{d_i}\right)^2 \hat{V}_{r,j}, \quad (2)$$

$$\Delta\hat{P}_{j,2} = (1 + \alpha_{j,2} - \gamma_o)\hat{V}_{j+1,2}^2 - (1 - \alpha_{j,2}) \times \hat{V}_{j,2}^2 + (\gamma_o + 2\alpha_{j,2})\hat{V}_{j,2}\hat{V}_{j+1,2}, \quad (3)$$

and

$$\hat{V}_{j+1,2} = \hat{V}_{j,2} + \left(\frac{d_r}{d_i}\right)^2 \hat{V}_{r,j}, \quad (4)$$

where the subscript j denotes the region under consideration (Fig. 1). The second subscript has values of 1 or 2 for the inlet and outlet manifold, respectively.

The following definitions are used in the above and following equations.

$$\hat{P} = \frac{P}{\rho V_i^2}, \quad \hat{V} = \frac{V}{V_i},$$

$$\alpha_{j,k} = \frac{1}{8} f_{j,k}\left(\frac{d_r}{d_i}\right)\left(1 - \frac{1}{4}\frac{d_r}{d_i}\right), \quad (5)$$

$$\Delta P_{j,k} = P_{j,k} - P_{j+1,k}, \quad k = 1, 2, \quad (6)$$

where $f_{j,k}$ is the Darcy friction factor corresponding to average branch velocity.

The terms γ_i and γ_o are pressure regain coefficients where

$$\gamma_i = \frac{V_{bj,1}}{V_{j,1}}, \quad \gamma_o = \frac{V_{bj,2}}{V_{j+1,2}}. \quad (7)$$

The pressure regain coefficient γ_i accounts for the transport of momentum from the manifolds to the risers. Likewise, γ_o accounts for momentum (in the direction of outlet fluid flow) transport from the risers to the outlet manifold. γ_i and γ_o are known for a given d_r/d_i ratio, riser tube spacing, and V_r (cf. Bajura and Jones[3]). Typically, γ_i is in the range of 0.8 to 1.1, and γ_o is about 0.

To determine the pressure distributions in the nonbranch regions (manifold lengths which have no side openings) of the manifold and in the risers, a modified Bernoulli equation is employed. For the nonbranch region the equations become in dimensionless form

$$\Delta\hat{P}'_{j,k} = \hat{P}_{j,k} - \hat{P}_{j+1,k} = \frac{1}{2} f'_{j,k}\left(\frac{w}{nd_i} - \frac{d_r}{d_i}\right)\hat{V}_{j,k}^2, \quad k = 1, 2, \quad (8)$$

where $f'_{j,k}$ is the Darcy friction factor in nonbranch regions of the manifold, based on velocity $\hat{V}_{j,k}$. For the riser the equation in dimensionless form becomes

$$\Delta\hat{P}_j^* = \frac{1}{2}\left(1 + k + f_{r,j}\frac{h_e}{d_r}\right)\mathrm{sgn}(\hat{V}_{r,j})\hat{V}_{r,j}^2. \quad (9)$$

The term k accounts for energy losses due to entrance and exit effects, $f_{r,j}$ is the Darcy friction factor based on the average velocity in the jth riser tube, and $\mathrm{sgn}(\hat{V}_{r,j})$ is +1 for upflow in the riser (i.e., $\hat{V}_{r,j} > 0$), and is −1 for downflow. In eqn (9) the pressure change due to hydrostatic head in nonhorizontal manifold systems has been ignored because it has no effect on the flow distribution.

All Darcy friction factors were evaluated by the implicit Colebrook equation (cf. White[23]) for flows in which $Re > 3000$, and were made equal to $64/Re$ for $Re < 2100$. In the transition regime they were obtained by linear interpolation between the value obtained from the Colebrook equation for $Re = 3000$ and the value of 64/2100. The relative roughness factor in the Colebrook equation was set midway between that for clean copper tubes and steel pipes.

Finally, since the pressure at any location within the dual-manifold system is single-valued, the net pressure change around any closed flow loop is zero. For parallel-flow dual-manifold systems this is expressed by

$$0 = \Delta\hat{P}_j^* - \Delta\hat{P}_{j+1}^* + \Delta\hat{P}'_{j+1,2} - \Delta\hat{P}'_{j+1,1} + \tfrac{1}{2}(\Delta\hat{P}_{j,2} + \Delta\hat{P}_{j+1,2} - \Delta\hat{P}_{j+1,1} - \Delta\hat{P}_{j,1}), \quad 1 \le j \le n - 1, \quad (10)$$

where the average pressure in a branch region is assumed to be the average of the pressures at the inlet and outlet of that branch. This is a reasonable assumption in light of the fact that the pressure distributions in the manifolds are linear in both branching and nonbranching regions, for any small distance in the flow direction (cf. Datta and Majumdar[9]).

Inspection of eqns (1)–(9) shows the flow distribution to be characterized by four dimensionless parameters, n, d_r/d_i, h_e/d_r, and w/nd_i. In addition, the flow rate at the inlet to the system also has some effect through the flow-rate-dependent friction factors in eqns (5), (8), and (9).

By inspection of eqns (1)–(9) it is possible to obtain insight into the effects of n, d_r/d_i, h_e/d_r, and w/nd_i on the flow distribution. For small d_r/d_i and n not large, the results presented in section 4 below show that uniform flow distribution is approached [since $\hat{V}_{r,j} \sim (1/n)(d_i/d_r)^2$, $1 \le j \le n$]. Inspection of eqn (9) shows that n and d_r/d_i enter the problem as n^2 and $(d_r/d_i)^4$, respectively. This leads to the expectation that in the range of parameters considered, flow distribution depends strongly on both n and d_r/d_i. The variable w/nd_i affects the problem only through the product $f'_{j,k}(w/nd_i - d_r/d_i)$ as indicated in eqn (8). Since $f'_{j,k}$ is typically on the order of 0.03, only large values of w/nd_i will make flow distribution sensitive to this parameter. The term h_e/d_r appears in eqn (9) as a product with $f_{r,j}$. The flow distribution is thus insensitive to h_e/d_r for $h_e/d_r < (1 + k)/f_{r,j} \approx 75$ at typical values of k and $f_{r,j}$. In most flat-plate collectors, however, h_e/d_r is normally at least 150, and hence, flow distribution depends strongly on h_e/d_r. The above qualitative observations will be revisited quantitatively below during the discussion of the results of this analysis.

Equations (1)–(4) and (8)–(10) compose a system of $(8n - 3)$ equations in $8n$ unknown quantities. The three additional equations needed are the boundary conditions

$$\hat{V}_{1,1} = 1, \tag{11}$$

and for parallel flow

$$\hat{V}_{1,2} = \hat{V}_{n+1,1} = 0. \tag{12}$$

For reverse flow, the latter two conditions are

$$\hat{V}_{n+1,2} = \hat{V}_{n+1,1} = 0. \tag{13}$$

The resulting system of nonlinear algebraic equations was solved numerically by the Newton–Raphson method with LU decomposition (Carnahan *et al.*[7]). The convergence criterion used was that the difference between two successive calculations of the riser flow rate had to be ≤0.1% for all risers.

All computations were performed on a 486 DX-33MHz personal computer. Typical run times were 1 min or less for manifold systems having eight risers.

3. MODEL AND PROGRAM VALIDATION

The model [eqns (1)–(9)] and its solution method are validated by comparing the numerical results with the data reported by Wang and Yu[21](no other experimental data were found). The experimental data are $n = 10$, $d_i = d_o = 13$ mm, $d_r = 6.5$ mm, $w = 30$ cm, $h_e = 1.12$ m, $\gamma_o = 0.0$, and $k = 1.0$. Coefficient γ_i was not given in the article by Wang and Yu[21], so a sensitivity analysis was performed for γ_i in the range of 0.8 to 1.1, recommended by McNown[17]and Pig-

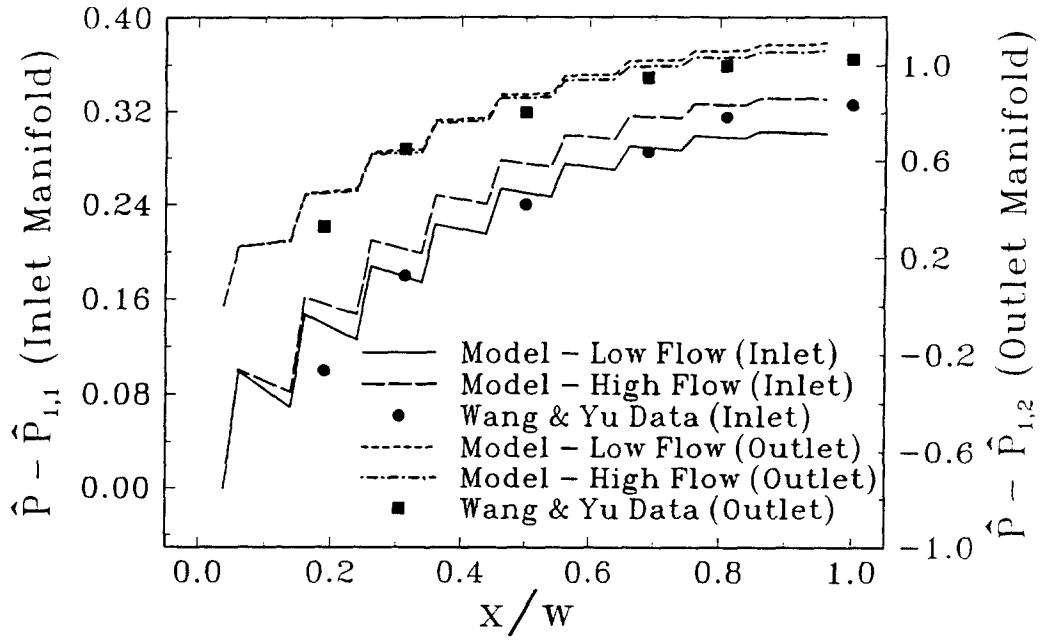

Fig. 3. Comparison of results from model with experimental data reported by Wang and Yu[21]. The flow rates are: Low flow = 1.89 l/min; high flow = 16.6 l/min.

ford *et al.*[19], and it was found that $\gamma_i = 1.1$ produced the best overall agreement with the experimental data. Since the total flow rate is also not reported in the study by Wang and Yu[21], and since it is known that the pressures in the manifolds are only weakly sensitive to total flow rates, we have made the computations for a low flow case of 1.89 ℓ/min and a high flow case of 16.6 ℓ/min in an attempt to at least provide results which bound the data. Figure 3 shows that the comparison between the thus-computed inlet and outlet manifold pressures and the experimental data is very good. The weak dependence on the total flow rate is indeed demonstrated in Fig. 3: a ninefold increase in total flow rate is seen to increase the manifold pressure by 10% at most. (After the completion of the study we have learned through personal communication with the senior author of the Wang and Yu[21]article that the flow rate used in their experiments was 6.4 ℓ/min, within the range of our computations presented in Fig. 3).

It is noteworthy that better overall agreement with experimental data would be obtained by allowing γ_i and k to vary with location along the manifolds. In most cases, however, this is unnecessary, since accuracy higher than that indicated in Fig. 3 is seldom sought.

4. RESULTS AND DESCRIPTION OF THE PHENOMENA

In addition to the above validation, the equations were solved for 54 different combinations of several of the independent variables for parallel (Z) and reverse (U) flow manifolds. The parameters for these cases were chosen to allow adequate insights into the nature of the fluid mechanics phenomena in this process, most particularly into the sensitivity of flow distribution to the major system variables. The various cases are listed in Table 1. The remaining variables were held constant at the following values: $d_i = d_o = 1$ in. (2.54 cm), $w = 3$ ft. (0.915 m), $h_e = 6$ ft. (1.83 m), $\gamma_o = 0.0$, $\gamma_i = 0.9$, and $k = 1.2$.

The ratio d_r/d_i, as seen in Table 1, was chosen to have the values 0.25, 0.50, and 0.75. Since h_e was fixed, it is to be noted that varying d_r changes not only d_r/d_i but also the ratio h_e/d_r. The sensitivity to inlet flow rate and temperature of the fluid was addressed here by varying the inlet Reynolds number (Re) as shown in Table 1. For example, $Re = 9640$ corresponds to a water temperature of 60°C and total flow rate of 1.89 ℓ/min.

Table 1. The computed cases

Case	d_r (cm)	n	Re	U or Z array
1	0.635	4	3210	Z
2	0.635	4	9640	Z
3	0.635	4	16100	Z
4	0.635	4	3210	U
5	0.635	4	9640	U
6	0.635	4	16100	U
7	0.635	8	3210	Z
8	0.635	8	9640	Z
9	0.635	8	16100	Z
10	0.635	8	3210	U
11	0.635	8	9640	U
12	0.635	8	16100	U
13	0.635	16	3210	Z
14	0.635	16	9640	Z
15	0.635	16	16100	Z
16	0.635	16	3210	U
17	0.635	16	9640	U
18	0.635	16	16100	U
19	1.27	4	3210	Z
20	1.27	4	9640	Z
21	1.27	4	16100	Z
22	1.27	4	3210	U
23	1.27	4	9640	U
24	1.27	4	16100	U
25	1.27	8	3210	Z
26	1.27	8	9640	Z
27	1.27	8	16100	Z
28	1.27	8	3210	U
29	1.27	8	9640	U
30	1.27	8	16100	U
31	1.27	16	3210	Z
32	1.27	16	9640	Z
33	1.27	16	16100	Z
34	1.27	16	3210	U
35	1.27	16	9640	U
36	1.27	16	16100	U
37	1.905	4	3210	Z
38	1.905	4	9640	Z
39	1.905	4	16100	Z
40	1.905	4	3210	U
41	1.905	4	9640	U
42	1.905	4	16100	U
43	1.905	8	3210	Z
44	1.905	8	9640	Z
45	1.905	8	16100	Z
46	1.905	8	3210	U
47	1.905	8	9640	U
48	1.905	8	16100	U
49	1.905	16	3210	Z
50	1.905	16	9640	Z
51	1.905	16	16100	Z
52	1.905	16	3210	U
53	1.905	16	9640	U
54	1.905	16	16100	U

A plot of the pressure distribution (referenced to an inlet pressure of zero) for the dual manifold system for cases 26 (Z-array) and 29 (U-array) described in Table 1 (in both cases $d_r/d_i = 0.5$, $n = 8$, $Re = 9640$) is shown in Figs. 4 and 5. To examine the hydrodynamics of the flow, we note that in the dividing (inlet) manifold the pressure rises during passage across a branch region due to the velocity reduction resulting from the removal of fluid from the manifold flow through the riser, such as from point a to b on the inlet manifold curve in Fig. 4. The pressure in the manifold decreases slightly due to frictional effects within the next part of the manifold which connects two branches, as seen in the transition from point b to c for the inlet manifold. In the combining (outlet) manifold, the addition of the riser tube flow accelerates the flow in the manifold and thus causes the pressure to decrease from point a to b along that combining branch. The pressure continues to drop between branch regions of the outlet manifold (from b to c), due to frictional losses. The pressure drop in each riser, and hence, the riser flow rate, can be determined from eqn (8) once the pressure distributions in each of the two manifolds are estab-

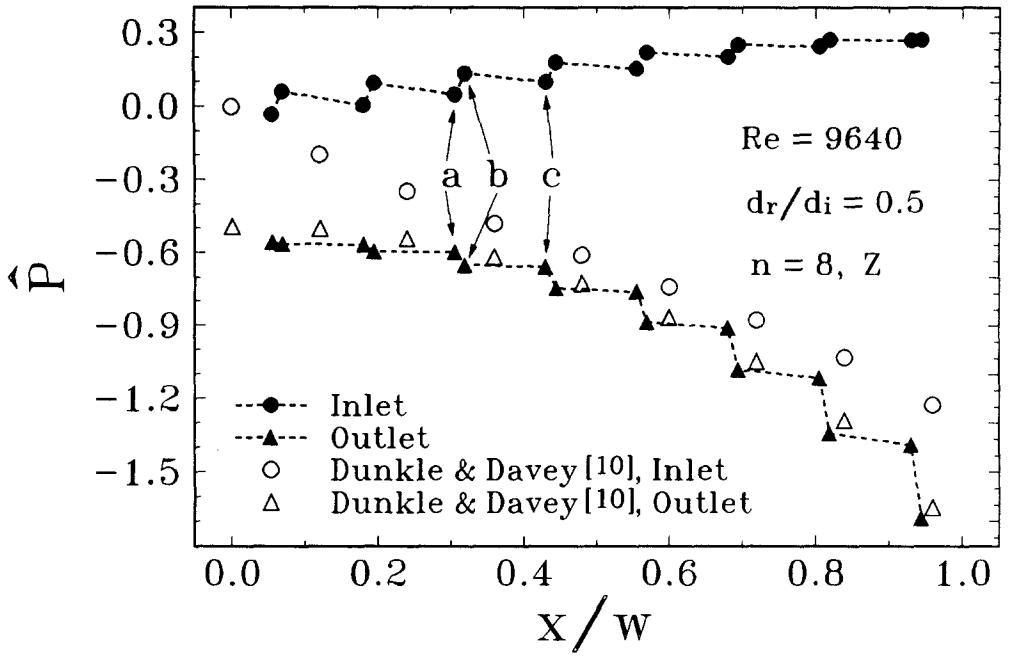

Fig. 4. Pressure distribution in the manifolds of the dual-manifold system, Z configuration, and comparison with results of the continuous model of Dunkle and Davey[10].

lished. As seen in Fig. 5, reverse-flow (U) manifold systems exhibit the same behavior.

The results in Figs. 4 and 5 are also compared with the closed-form solutions from the continuous models of Dunkle and Davey[10]and Bassiouny and Martin[5]. In their analyses, the former neglected inertial pressure changes in the manifolds (only friction was included) and the latter authors neglected friction (only inertia was included). By inspection, it is clear that the neglect of inertia causes a gross underprediction of the pressure distribution in the inlet manifold (Fig. 4), whereas the neglect of friction produces less inaccuracy (Fig. 5) for the example considered here. The inertial model of Bassiouny and Martin[5]overpredicts riser flows near $x/w = 1$ by about 35%.

Figs. 6 and 7 show the dimensionless flow rate ($\hat{Q}_j$) distribution among the risers, for $d_r/d_i = 0.25$ and 0.75, respectively, for Z and U configurations, and

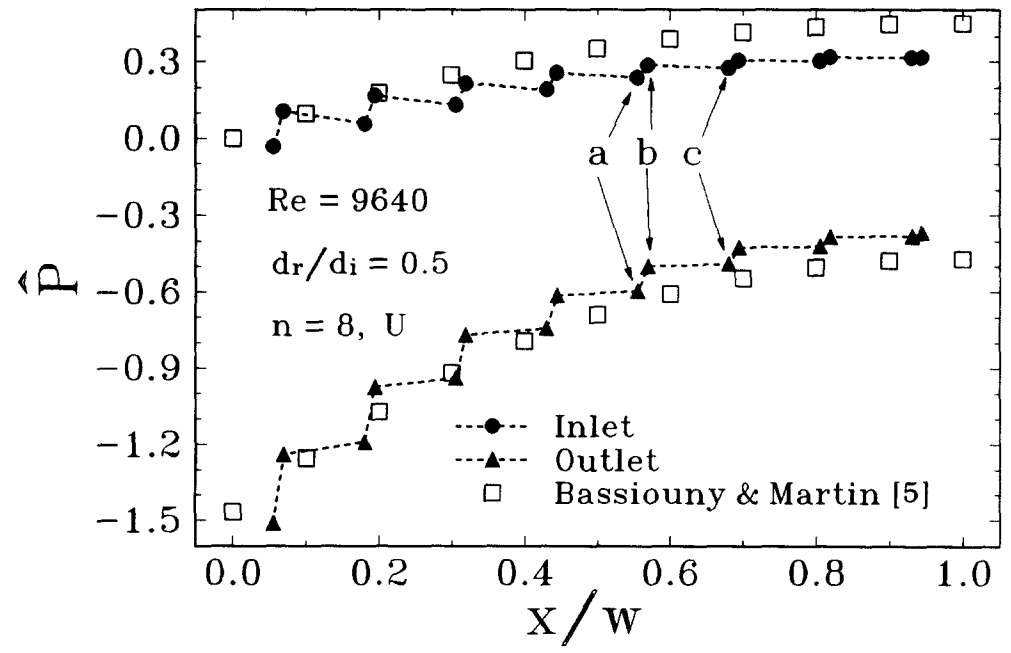

Fig. 5. Pressure distribution in the manifolds of the dual-manifold system, U configuration, and comparison with the results of the continuous model by Bassiouny and Martin[5].

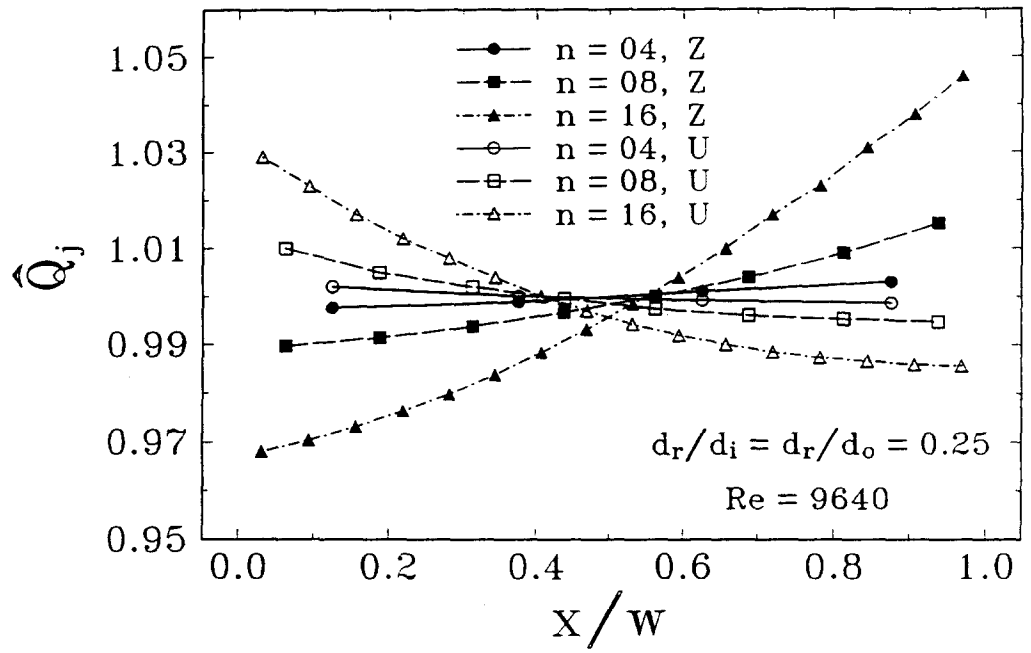

Fig. 6. Distribution of riser flow rates for $d_r/d_i = 0.25$.

$Re = 9640$. It should be noted that the extent of the deviation of $\hat{Q}_j$ from unity is a measure of maldistribution, with values above 1 indicating higher-than-average flow and values below 1 indicating lower-than-average flow.

Inspection of Fig. 6 (in which $d_r/d_i = 0.25$) shows that maldistribution in this case is small and increases with the number of risers. Maximal riser flow rates are observed to be 5% above average, occurring in the end riser (nearest to $x/w = 1$) for the Z configuration, and 3% above average in the first riser (nearest to $x/w = 0$) for the U configuration. Both maxima are at the highest number of risers considered in this figure, $n = 16$. For both array configurations the flow rates in the risers are observed to change monotonically with riser location along the manifold. The trend in which the highest riser flow occurs in the risers furthest from the entrance ($x/w = 1$) for the Z configuration and nearest to the entrance ($x/w = 0$) for the U configuration is consistent among all the cases investigated here. This

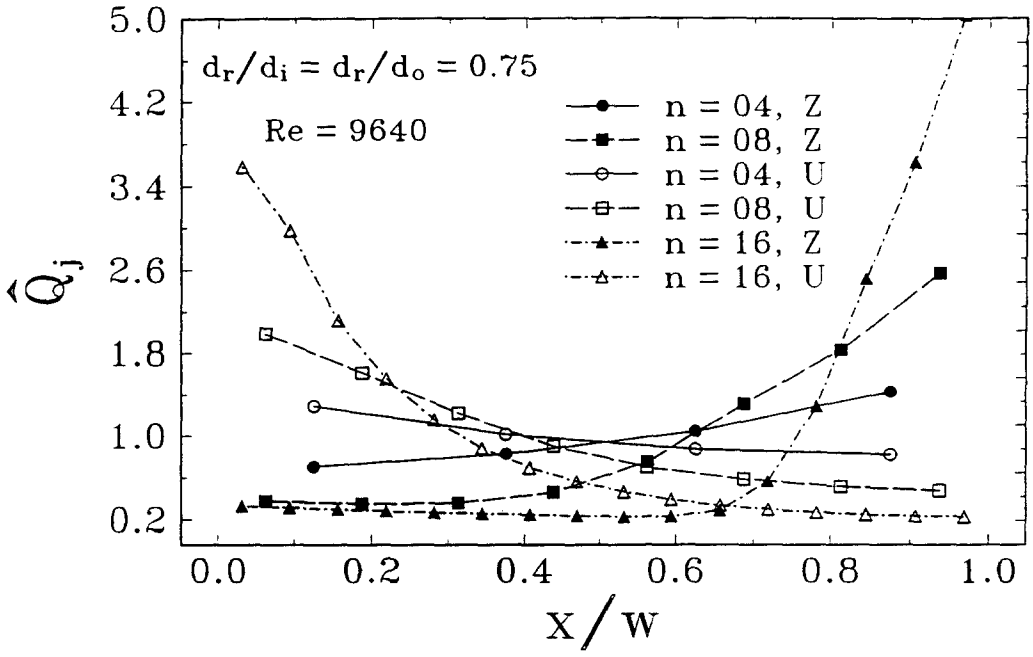

Fig. 7. Distribution of riser flow rates for $d_r/d_i = 0.75$.

behavior is also consistent with the manifold pressure distributions shown in Figs. 3 and 4: for the Z configuration, the pressure in the inlet manifold increases, and that in the outlet manifold decreases with increasing x/w. This results in an increasing pressure difference across each riser, from the one closest to the manifold inlet to the one furthest from it. Equation (9) shows that this increase in pressure difference results in the observed increase in riser flow rate. For the U configuration there is a pressure increase along both manifolds, but it is much more pronounced in the outlet manifold, causing the manifold pressure distributions to converge with increased x/w and thus reduce the riser flow rates in that direction.

For $d_r/d_i = 0.75$, Fig. 7 shows the same flow trends as above, but the extent of flow maldistribution is greatly increased, reaching riser flows which differ about fivefold from the average. This is brought about by the fact that the large increase in the riser diameter decreases the frictional pressure drop across the risers [as seen from the consequence of the decreased magnitude of the term h_e/d_r in eqn (9)], leaving the pressure field in the system to be strongly affected by the nonlinear inertial effects in each manifold [eqns (1) and (3)] which are in this case not sufficiently moderated by the flow resistance in the risers.

This effect of the pressure change in the risers on the flow distribution is clarified as follows. The orders of magnitude of the different pressure drops in the manifold system, shown in eqn (10) are first estimated. The nonbranch region pressure drops $\Delta\hat{P}'_{j+1,2}$ and $\Delta\hat{P}'_{j+1,1}$ depend strongly on w/nd_i [see eqn (8)] and are on the order of 0.1 for typical solar collectors. The pressure drops across each manifold branch region, $\Delta\hat{P}_{j,2}$, $\Delta\hat{P}_{j+1,2}$, $\Delta\hat{P}_{j+1,1}$, and $\Delta\hat{P}_{j,1}$, calculated from eqns (1) and (3), are all at most on the order of unity and typically smaller, since all the terms on the right-hand side of these equations are of this order. The order of the riser pressure drop terms $\Delta\hat{P}^*_j$ and $\Delta\hat{P}^*_{j+1}$ is examined by combining eqns (9) and (2), resulting in

$$\Delta\hat{P}^*_j = C_j\left(\frac{d_r}{d_i}\right)^{-4}(\hat{V}_{j+1,1} - \hat{V}_{j,1})^2 \equiv C_j\left(\frac{d_r}{d_i}\right)^{-4}\Delta\hat{V}^2_{j,1}, \tag{14}$$

where

$$C_j = \frac{1}{2}\left(1 + k + f_{r,j}\frac{h_e}{d_r}\right)\mathrm{sgn}(\hat{V}_{r,j}). \tag{15}$$

Equation (14) shows that $\Delta\hat{P}^*_j$, the pressure drop in the risers, can become significantly larger than the other above-evaluated pressure-drop terms in the branch and nonbranch regions in eqn (10), if C_j is large and d_r/d_i is of the order of 1 or less, or even if only $d_r/d_i \ll 1$. Equation (10) is then satisfied by the condition

$$\Delta\hat{P}^*_{j+1} \approx \Delta\hat{P}^*_j, \quad 1 \le j \le n-1, \tag{16}$$

which from eqn (9) implies uniform flow distribution. For this case, $\Delta\hat{V}_{j,1} \approx 1/n$, and eqn (14) becomes

$$\Delta\hat{P}^*_j \approx C_j\left(\frac{d_r}{d_i}\right)^{-4} n^{-2}. \tag{17}$$

This result prompted Bajura and Jones[3]and Datta and Majumdar[9]to correlate results against a single area ratio parameter $n(d_r/d_i)^2$.

C_j becomes large when h_e/d_r is large. For example, $h_e/d_r = 200$ gives a C_j of about 5 and a $\Delta\hat{P}^*_j$ on the order of 1 or larger, indeed causing the $\Delta\hat{P}^*_j$ terms to be predominant in eqn (10).

A general conclusion from this discussion is that if the riser pressure drops are not the predominant terms in eqn (10), eqn (16) would not be satisfied and maldistribution would thus occur. For both C_j and d_r/d_i near 1, eqn (14) reveals that $\Delta\hat{P}^*_j$ is of the order of $\Delta\hat{V}^2_{j,1}$. Comparing the orders of $\Delta\hat{P}^*_j$ and the manifold pressure drop terms at a branch, say $\Delta\hat{P}_{j,1}$, by taking the ratio of eqns (14) and (1) (assuming for simplification that $\gamma_i = 1$ and $\alpha_{j,1} = 0$), this ratio is

$$\frac{\Delta\hat{P}^*_j}{\Delta\hat{P}_{j,1}} = C_j\left(\frac{d_r}{d_i}\right)^{-4}\left(1 - \frac{\hat{V}_{j,1}}{\hat{V}_{j+1,1}}\right). \tag{18}$$

For C_j and d_r/d_i near 1, eqn (18) indicates that the pressure ratio $\Delta\hat{P}^*_j/\Delta\hat{P}_{j,1}$ is less than the order of 1, since the velocities in adjacent risers do not differ by too much. Consequently, eqn (10) would not lead to the condition of eqn (16), and maldistribution will occur.

For the Z array, the constraint of zero velocity in the inlet manifold at $x/w = 1$ produces $\Delta\hat{V}_{n,1}$ [and through eqn (14), also $\Delta\hat{P}^*_n$] of the order of one: the largest in the system. To satisfy eqn (10), $\Delta\hat{P}^*_{n-1}$ must be of similar order, though slightly smaller than $\Delta\hat{P}^*_n$ because of the inertially caused pressure increases at the n and $n-1$ branches of the inlet manifold. From eqn (9), it can be seen that this results in maximal riser flow in riser tube n with the riser flow decreasing nearly monotonically with distance toward the entrance to the inlet manifold (Fig. 7). For $n = 16$, the existence of the large numbers of flow-starved risers due to small $\Delta\hat{P}^*_j$ gives rise to the large flow imbalance reflected in Fig. 7 for this case.

Dual-manifold systems characterized by manifold inertia effects comparable to those of riser friction, with riser flow distributions shown in Fig. 7, are called "inertially dominant," whereas those of Fig. 6, where riser friction is most significant, are called "frictionally dominant." These conclusions, including the fact that riser maldistribution is decreased when the pressure drop in the risers becomes dominant, and the specific role of h_e/d_r in controlling maldistribution, agree with past studies[10,12,13,15].

The influence of the inlet Reynolds number on maldistribution, as shown in Figs. 8 and 9, is weak: a fivefold increase of Re (from 3210 to 16,100) increased the maximal flow rate in the riser by about 5% and

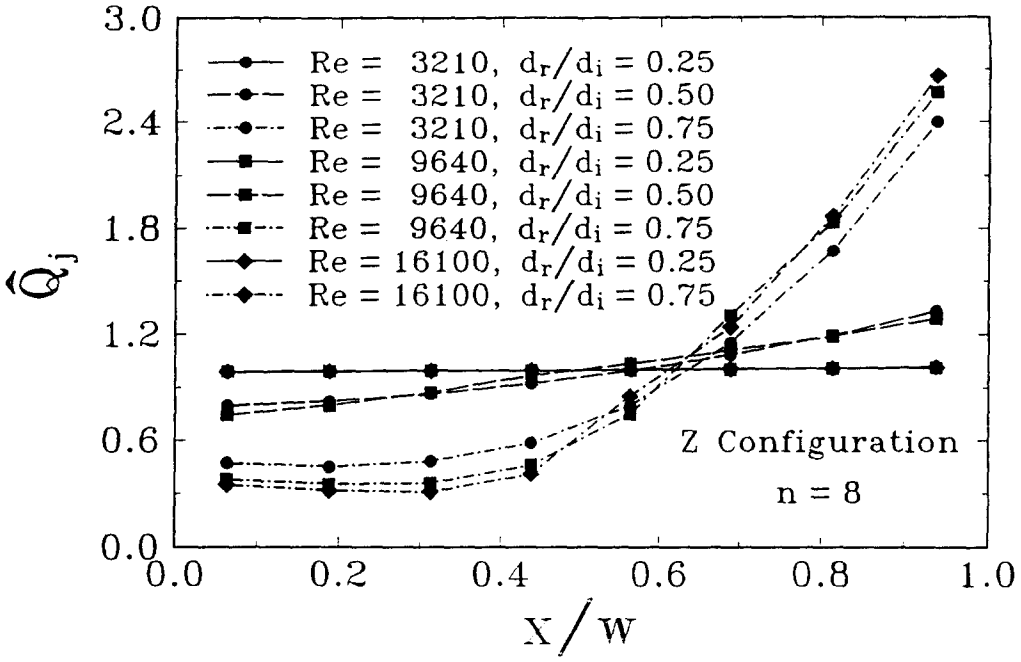

Fig. 8. Effect of dual-manifold system inlet Reynolds number (*Re*) on the distribution of riser flow rates, Z configuration.

decreased the minimal flow rate by about the same amount.

5. CONCLUSIONS

For the system geometry considered and the range of parameters investigated in this article, the following conclusions are obtained.

1. An effective model for predicting flow and pressure distribution in dual-manifold systems characteristic to solar collectors was developed and validated by comparison to available experimental data. Computation time on a 486DX-33MHz personal computer is of the order of 1 min.
2. For the parallel flow (Z) configuration the riser flow rate increases from riser to riser in the manifold

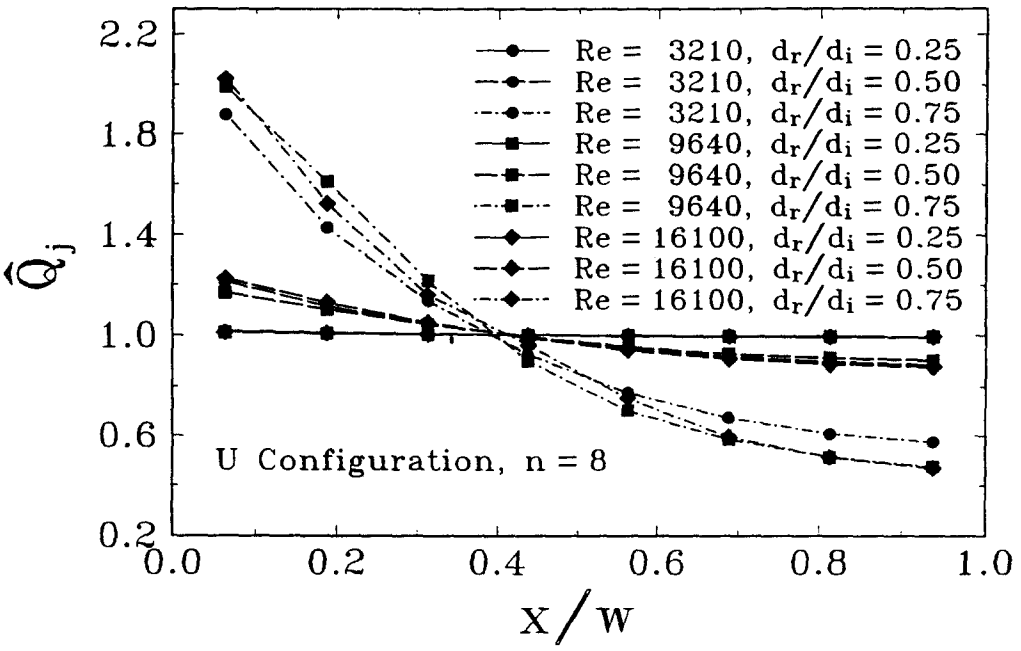

Fig. 9. Effect of dual-manifold system inlet Reynolds number (*Re*) on the distribution of riser flow rates, U configuration.

flow direction. It is thus lowest at the entrance to the inlet manifold and highest at the outlet from the outlet manifold. The opposite occurs in the reverse flow (U) configuration.

3. The ratio of riser to manifold diameters (d_r/d_i) has a major influence on flow maldistribution in typical solar collectors, increasing as $(d_r/d_i)^4$. Values of d_r/d_i as small as practicable should thus be employed to make the flows through the risers as equal as possible and thus increase the thermal efficiency of the collector.
4. The second major influence on riser flow distribution is the number of risers, n. Maldistribution increases with n^2. For example, for $d_r/d_i \leq 0.25$, dual-manifold systems having as many as 16 riser tubes will operate with peak riser flows 5% greater than average, whereas for $d_r/d_i = 0.50$, only the systems having eight risers or less would have a peak riser flow limited to about 30% greater than average. For $d_r/d_i = 0.75$, peak riser flows 500% greater than average can occur in the parallel flow configuration.
5. The effect of the distance between the risers $[w/(nd_i)]$ (which varied here between 2.25 and 4.00) is generally weak for systems having values h_e/d_r of 48 to 144 used in this study, since $w/(nd_i)$ enters the problem only as a product with a small-valued friction factor.
6. Decreasing the ratio h_e/d_r increases maldistribution because it decreases the role of frictional pressure changes within the risers. For h_e/d_r less than about 75, pressure changes in the system arising from inertia in the manifolds and friction in the risers are of similar magnitudes, giving rise to large flow maldistribution. This effect is most pronounced for d_r/d_i ratios approaching 1.
7. For the parallel-flow configuration, it is clearly demonstrated from the mathematics of the discrete formulation and as a consequence of the imposed boundary conditions, that the risers farthest from the inlet experience the greatest flows in general. As a limiting case, the mathematics further show that the flow distribution tends toward uniformity as pressure drops in the risers become large relative to the inertial and frictional pressure changes in the manifolds.

Acknowledgment—The origins of this study were partially supported by the USDOE, Solar Heating and Cooling R & D Branch.

NOMENCLATURE

- C dimensionless coefficient, eqn (14)
- d inside diameter of tube, m
- f Darcy friction factor in branch region, based on average branch velocity, dimensionless
- f' Darcy friction factor in nonbranch region of manifold, dimensionless
- h_e length of riser, m
- k entrance and exit energy loss coefficient, dimensionless
- ℓ length of control volume for momentum balance, m
- n number of risers
- P pressure, Pa
- $\hat{P}$ dimensionless pressure, eqn (5)
- $\dot{Q}_j$ volumetric flow rate in riser, ℓ/min
- $\dot{Q}_T$ total volumetric flow rate to the dual-manifold system, ℓ/min
- $\hat{Q}_j$ dimensionless flow rate in riser, $\dot{Q}_j/(\dot{Q}_T/n)$
- Re Reynolds number at the inlet to the dual manifold system, based on d_i, dimensionless
- V fluid velocity, m/s
- V_i fluid velocity at entrance to inlet manifold, m/s
- V_b velocity component leaving or entering an inlet or outlet manifold to or from a branch, m/s
- $\hat{V}$ dimensionless velocity of fluid, eqn (5)
- w total width of dual-manifold system, m
- x coordinate in direction of flow along inlet manifold, m

Greek

- α coefficient in eqn (5), dimensionless
- γ pressure regain coefficient, dimensionless
- ρ density, kg/m^3
- τ shear stress, N/m^2

Subscripts

- i dividing (inlet) manifold
- o combining (outlet) manifold
- j refers to a region of the dual-manifold system (Fig. 1)
- k $k = 1$ refers to inlet manifold, $k = 2$ to outlet manifold
- r riser

Superscripts

- $'$ refers to pressure change in a nonbranch region of a manifold
- $*$ refers to pressure change in a riser

REFERENCES

1. A. Acrivos, B. D. Babcock, and R. L. Pigford, Flow distributions in manifolds, *Chem. Eng. Sci.* **10,** 112 (1959).
2. R. A. Bajura, A model of flow distribution in manifolds, *ASME J. Eng. Power* **93,** 7 (1971).
3. R. A. Bajura and E. H. Jones Jr., Flow distribution manifolds, *ASME J. Fluids Eng.* **98,** 654 (1976).
4. C. A. Bankston (ed.), *Proc. International Energy Agency Workshop on the Design and Performance of Large Solar Thermal Collector Arrays,* San Diego, CA, Solar Energy Research Institute Report SERI/SP-271-2664 (June 1984).
5. M. K. Bassiuony and H. Martin, Flow distribution and pressure drop in plate heat exchangers—I. u-type arrangement, *Chem. Eng. Sci.* **39**(4), 693–700 (1984).
6. M. K. Bassiuony and H. Martin, Flow distribution and pressure drop in plate heat exchangers—II. z-type arrangement, *Chem. Eng. Sci.* **39**(4), 701–704 (1984).
7. B. Carnahan, H. A. Luther, and J. O. Wilkes, *Applied numerical methods,* Wiley, New York (1969).
8. J. P. Chiou, The effect of nonuniform flow distribution on the thermal performance of solar collectors, *Solar Energy* **29,** 486–502 (1982).
9. A. B. Datta and A. K. Majumdar, Flow distribution in parallel and reverse flow manifolds, *Int. J. Heat Fluid Flow,* **2**(4), 253–262 (1981).
10. R. V. Dunkle and E. T. Davey, Flow distribution in solar absorber banks, *Proc. ISES Conf.,* Paper 4/35, Melbourne, Australia (March 1970).
11. W. H. Hager, Flow in distribution conduits, *Proc. Inst. Mech. Engrs.* **200,** 205–213 (1986).
12. G. F. Jones and N. Lior, Isothermal flow distribution in solar collectors and collector manifolds, *Proc. Annual*

Meeting AS/ISES, Denver, CO, Vol. 2.1, pp. 362–372 (August 1978).

13. G. F. Jones and N. Lior, Conjugate heat transfer and flow distribution in an assembly of manifolded finned tubes. In: J. B. Kitto Jr. and J. M. Robertson (eds.), *Maldistribution of flow and its effect on heat exchanger performance,* ASME HTD Vol. 75, pp. 127–136 (1987).
14. G. F. Jones, Consideration of the heat-removal factor for liquid-cooled flat plate solar collectors, *Solar Energy* **38,** 455–458 (1987).
15. D. S. Knowles, A simple balancing technique for liquid cooled flat plate solar collector arrays, *Proc. AS/ISES Conf.,* Vol. 3.1, 300–303 (1981).
16. N. Lior, Thermal theory and modeling of solar collectors, In: F. de Winter (ed.), *Solar collectors, energy storage, and materials,* MIT Press, Cambridge, MA, pp. 99–182 (1991).
17. J. S. McNown, Mechanics of manifold flows, *Trans. ASCE* **110,** 1103–1142 (1954).
18. Y. Menuchin, S. Bassler, G. F. Jones, and N. Lior, Optimal flow configuration in solar collector arrays, *Proc. Annual Meeting AS/ISES,* Philadelphia, PA, Vol. 4.1, pp. 616–620 (May 1981).
19. R. L. Pigford, M. Ashraf, and Y. D. Miron, Flow distribution in piping manifolds, *Ind. Eng. Chem. Fundam.* **22,** 463–471 (1983).
20. P. I. Shen, The effect of friction on flow distribution in dividing and combining flow manifolds, *ASME J. Fluids Eng.* **114,** 121–123 (1992).
21. X. A. Wang and P. Z. Yu, Isothermal flow distribution in header systems, *Int. J. Solar Energy* **7,** 159–169 (1989).
22. X. A. Wang and L. G. Wu, Analysis and performance of solar collector arrays, *Solar Energy* **45,** 71–78 (1990).
23. F. M. White, *Fluid mechanics,* McGraw-Hill, New York (1986).